Engineering Structures 238 (2021) 112276

Contents lists available at ScienceDirect

Engineering Structures

journal homepage: www.elsevier.com/locate/engstruct

Testing and evaluation of web bearing capacity of corroded steel bridge girders

Amanda Bao [a,*], Caleb Guillaume [b], Christopher Satter [b], Alana Moraes [b], Peter Williams [b], Tucker Kelly [b], Ying Guo [c]

[a] Rochester Institute of Technology, 78 Lomb Memorial Drive, ENT-3154, Rochester, New York 14623, USA
[b] Rochester Institute of Technology, 78 Lomb Memorial Drive, CETEMS, Rochester, New York 14623, USA
[c] Rochester Institute of Technology, 78 Lomb Memorial Drive, Rochester, New York 14623, USA

ARTICLE INFO

Keywords:
Web bearing
Corrosion
Steel
Bridge

ABSTRACT

Aging bridges have become an important issue in the United States. One of the most dominant forms of deterioration for steel bridges is corrosion, which is typically due to moisture exposure and water leakage through deck joints. In cold regions, frequent use of deicing chemicals during the winter season further contributes to the corrosion process. Over the years, corrosion can become serious enough to disconnect the girder's web from its flanges. This excessive rust accumulation and metal area loss pose significant concerns for the reduction of the structural capacity of a girder, especially at its ends. In this paper, new corroded sample preparation and testing procedures were developed and implemented to study the residual web bearing capacity of corroded steel beam specimens in the lab. The laboratory testing results were used to extend the study to evaluate the residual web bearing capacity of corroded steel bridge girders. Corroded steel beam specimens were approximated in two forms in laboratory testing. In the first form, web thinning was achieved by prolonged submersion in bleach solution, to develop surface corrosion and section loss. In the second form, web holes were cut out of specimens with a plasma torch. Loading tests were performed on scaled steel beam specimens to investigate the consequent reduction in web bearing capacity due to web thinning and web area losses. The reaction at girder ends was simulated by a compression force exerted on the top flange of the steel beam specimens through a loading plate of the Material Testing System. The residual strengths of the steel beam specimens, varying in levels of corrosion, were analyzed and compared with the 3-D finite element modeling results. A quantitative relationship between corrosion condition and residual web bearing strength of I-plate steel girders is developed based on the laboratory testing and numerical modeling results. The findings in this study align with the observations from the real-world bridge practice. The proposed table of web bearing strength reduction factors can be used as a reference for evaluating residual web bearing capacity of corroded steel girders in bridge loading rating.

1. Introduction

According to the United States 2016 National Bridge Inventory [10] database, almost 20% of all the steel bridges in the US were rated structurally deficient. As a result, aging infrastructure has been receiving increased attention. Bridge deterioration is mainly caused by repeated vehicular loads and adverse environmental exposure. Corrosion is the most dominant deterioration form for steel bridges [14]. Moisture exposure and leakage of water through deck joints are the main causes of steel bridge corrosion. In cold regions, frequent use of deicing chemicals during the winter season further accelerates the corrosion process. Many steel multi-girder bridges in the United States display severe corrosion forms, generally at the girder ends below deck joints and along the lower portions of the girder webs. Over the years, some corrosion can be severe enough to have the lower web disconnect from the bottom flange for a length up to a few meters near the girder ends, as shown in Fig. 1 [3]. In Fig. 1, the two images on the top show the localized rust-through corrosion at the girder web near the bottom flanges, and the two images in the middle demonstrate significant amount of rust accumulated at the girder ends due to leakage of liquid through deck joints, and the

* Corresponding author at: Rochester Institute of Technology, 78 Lomb Memorial Drive, ENT-3154, Rochester, New York 14623, USA.
E-mail addresses: axbite@rit.edu (A. Bao), cjg4192@rit.edu (C. Guillaume), cds5494@rit.edu (C. Satter), axm2553@rit.edu (A. Moraes), pjw9867@rit.edu (P. Williams), txk9156@rit.edu (T. Kelly), guoying0829@163.com (Y. Guo).

https://doi.org/10.1016/j.engstruct.2021.112276
Received 15 June 2020; Received in revised form 14 March 2021; Accepted 21 March 2021

images on the bottom illustrate the typical locations of rust along the girder lower web and at the girder ends.

This paper is focused on the analysis and evaluation of web bearing capacity of deteriorated steel girder bridges in poor and severe conditions, and intends to provide technical support to the current bridge load rating practice. Limited research on the issues relating to the behaviors and strength of deteriorated steel girder bridges has been done in the past 30 years. Fernandez et al. stated that corrosion was one of the most noteworthy degradation mechanisms in steel structures and pitting corrosion had a strong effect on the fatigue life of steel structures [5]. Nishikata et al. pointed out that steel structures encountered difficulties in coastal areas, because airborne salt deposits may generate porous and non-adhesive rusts on the surface [12]. Parameter analysis on weathering steel corrosion was performed and its applications to bridges was investigated by Guo et al. [7]. Researchers from Rochester Institute of Technology conducted 3-D numerical modeling of deteriorated steel girder bridges and analyzed the structural capacity of corroded girders [3,4]. Michigan Technological University researchers developed guidelines for steel beam end deterioration [16]. Kayser et al. developed a damage model which evaluates the reliability of a corroded steel girder over time [8]. Researchers from the City College of New York developed deterioration curves and equations using the Weibull-based method to calculate deterioration rates for bridge elements [1]. Ghosn et al. developed a Load and Resistance Factor Rating methodology to evaluate New York State bridges in the US [6]. Appuhamy et al. developed an assessment method and a maintenance management strategy based on the results of tensile coupon tests conducted on corroded plates obtained from a steel plate girder serviced 100 years with severe corrosion [2]. Most of the prior research work on steel girder bridge corrosion was theoretical and numerical, and few lab testing and/or field testing were performed to validate the numerical modeling results due to the difficulty in handling the large scale structure, extreme long time duration for preparing steel girder corrosion specimens and the uncertainty in controlling corrosion forms in a lab setting. In order to bridge the research gap, new corroded sample preparation and testing procedures were developed and implemented in this study. The new corrosion preparation and testing procedure made it feasible to test the residual web bearing capacity of corroded steel beam specimens in the lab. After calibrating the numerical models by the first-hand laboratory testing results for the steel beam specimens, large scale numerical modeling can be implemented to extend the study to evaluate the residual web bearing capacity of real-world corroded steel bridge girders.

In this paper, the residual web bearing strength of deteriorated steel bridge girders with different corrosion conditions is investigated by laboratory testing and numerical modeling. The failure mode in this study is focused on web bearing buckling failure, which is characterized by significant out-of-plane displacement perpendicular to the load direction due to the increased web depth-to-thickness ratio caused by the reduction of web thickness as a result of corrosion. At the end of the paper, recommended values of web bearing strength reduction factors accounting for different degrees of section losses are proposed based on the testing and modeling results.

2. Lab testing

2.1. Sample description

W8x10 steel beam specimens were tested in a lab setting to investigate the web bearing capacity under different corrosion forms and conditions. The sample size W8x10 was selected based on careful consideration of different factors including the depth-to-thickness ratio of web close to that of real bridge girders, feasibility and ease of

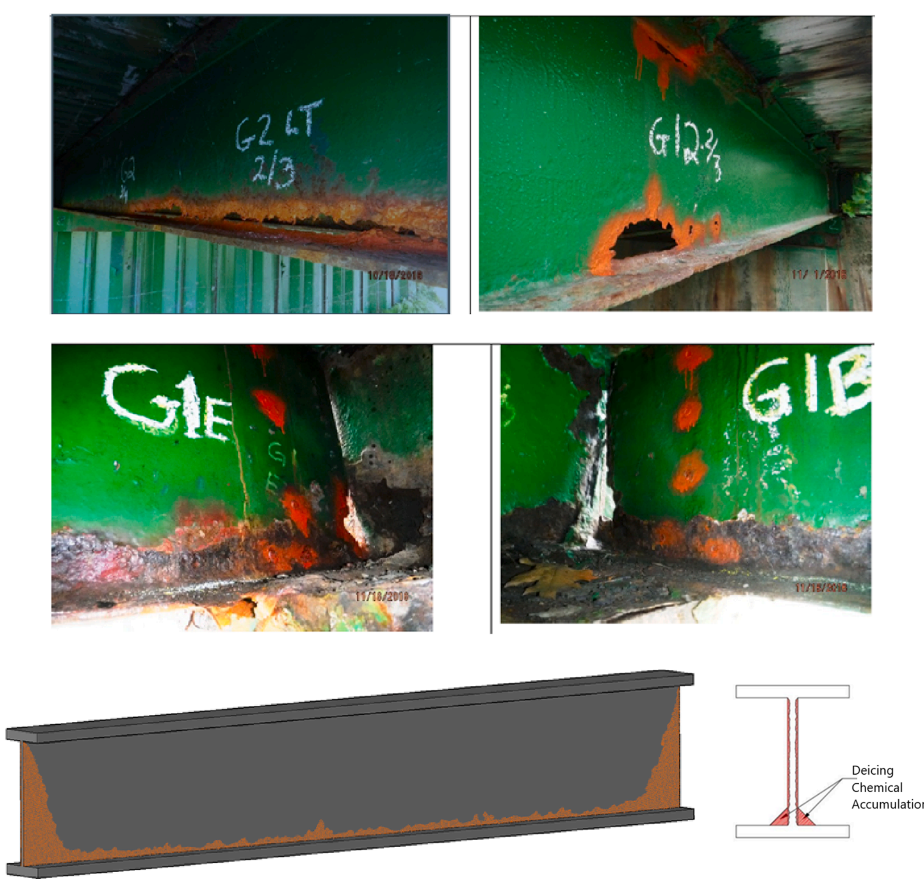

Fig. 1. Typical Locations and Forms of Steel Girder Bridge Corrosion [3].

handling of the corrosion development procedure in lab and the loading limit of the testing machine to reach the web buckling strength of the steel beam specimens. The lab testing was aimed at the effect of different corrosion forms and corrosion levels on the residual web bearing strength of steel beam specimens, and the lab testing results were used to calibrate the finite element models, which can be projected to predict the performance of large-scale steel bridge girders under the similar corrosion conditions. The hot rolled W8x10 steel beam specimens were purchased from a local steel supplier. Dimensions and section properties of a typical W8x10 beam are listed in Table 1 and the W8x10 beam specimens used in this study were the standard hot-rolled shapes having the typical dimensions within standard fabrication tolerances. The initial web depth-to-thickness ratio of the W8x10 beam specimens was 40.5, which has the largest depth-to-thickness ratio among all the standard W8x beams. The mechanical properties are provided by the steel fabricator according to the American Society for Testing and Materials (ASTM) testing standard. The W8x10 steel beams used in this study have the yield strength of 345Mpa (50ksi), the ultimate strength of 448Mpa (65ksi), and the elastic modulus of 200Gpa (29,000ksi). Each steel beam specimen was factory-cut at 15.2 cm (6 in.) long and shipped to the lab with the starting surface condition of rust-free, and the beam specimens were thoroughly washed to remove any oils or stains.

2.2. Sample preparation

The W8x10 steel beam specimens were submerged in plastic containers filled with 6.0% sodium hypochlorite bleach to develop surface corrosion, as shown in Fig. 2. In order to restrict the rust to the beam web area, corrosion resistant rubberized undercoating was used to protect the flanges. To maximize coating adhesion, specimens were thoroughly scrubbed with steel brushes to remove initial rust and imperfections, and then scrubbed with nylon brushes and acid wash to remove all oils and foreign debris. Once clean and fully dried, the specimen's initial mass and web thickness were measured and recorded. The web thickness was taken at quarter points along the web depth and then averaged. Three layers of rubberized coatings were applied to the flanges of beam specimens. The drying time between each coating was 60 min. After the final coating, the specimens were dried for at least 24 h, before being submerged into bleach solutions. The actual soaking times varied from 7 days to 36 days, in order to develop different degrees of corrosion.

Once the desired amount of rust was developed according to the measured remaining web thickness, the beam specimens were removed from the plastic container. The protective flange coatings were removed using a putty knife. The corrosion byproduct was scrubbed off with a steel brush. Then, the steel beam specimens were water washed and dried. Post-corrosion measurements of the beam specimens' mass and the web thickness were taken and recorded. Due to variations of corrosion and surface roughness on the web during soaking, the web thickness was averaged along the web depth at quarter points, and the coefficients of variation were ranging from 5% to 11% for the web thickness measurement along the web depth of steel beam specimens. In this study, the beam specimen weight loss was assumed to be due to web corrosion only, and the web thickness loss was calculated based on the weight loss and verified by the web thickness measurement.

Three types of beam corrosion were simulated: web thinning due to rust, a localized hole through the web, and a combination of the two. Web thinning was achieved by soaking the specimens in bleach solution, as described previously. Web holes, as shown in Fig. 3, were obtained by cutting the area of the hole out of the web using a plasma torch. The specimens of the combined web thinning and hole were obtained by cutting material from the web of specimens that were previously soaked in bleach solution. The description of the steel beam specimens used for lab testing is listed in Table 2.

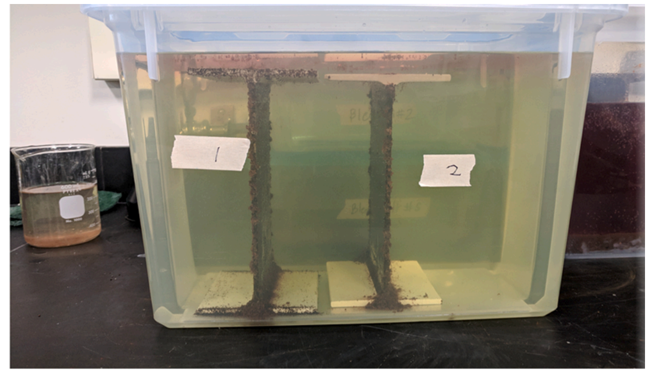

Fig. 2. Soaking Beam Specimens into Bleach Solution.

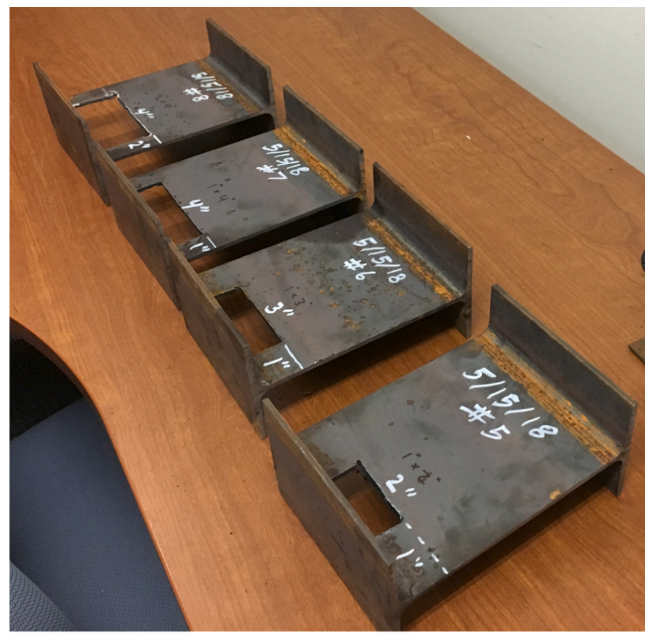

Fig. 3. Beam Specimens with Hole Cut out of the Web.

2.3. Testing procedure

The beam specimens were labeled with a test date, a model number, reference lines for lateral displacement measurements, and the dimensions of the hole if applicable. Compression tests on the sample beams were performed using the Material Testing System, which has a loading limit of 200 kN (45 kips). The compression force was applied on the top flange of the steel beam specimen, and the direction of the compression force was perpendicular to the beam length and parallel to the web depth, which simulated the vertical reaction at the beam end in the real-world structure. The loading rate was controlled at 0.0254 mm

Table 1
Dimensions and Properties of W8x10.

Shape	Area (cm^2)	Depth (cm)	Web thickness (cm)	Flange width (cm)	Flange thickness (cm)	Weight (kg/m)	Web h/t_w ratio	Moment of inertia I_x (cm^4)	Moment of inertia I_y (cm^4)
W8x10	19.1	20	0.43	10	0.52	14.9	40.5	1282	87

Table 2
Lab Testing Steel Beam Specimens Description.

Group No. Corrosion Form	1 Web Thinning (Thickness Loss)			2 Web Hole Only Hole Size (Height × Length): cm × cm						3 Web Thinning + Web Hole Average Thickness Loss: 8.7% Hole Size (Height × Length): cm × cm					
Condition	0 %	8.7 %	14.8 %	2.54 x 5.08	2.54 x 7.62	2.54 x 10.2	5.08 x 5.08	5.08 x 7.62	5.08 x 10.2	2.54 x 5.08	2.54 x 7.62	2.54 x 10.2	5.08 x 5.08	5.08 x 7.62	5.08 x 10.2
No. of Samples	3	3	3	3	3	3	3	3	3	3	3	3	3	3	3
Lab Data Plot	Fig. 7			Fig. 8						Fig. 9					

per second (0.001 in. per second). Testing software connected to the testing machine was used to automatically collect testing data and produce force versus vertical displacement curves. The vertical displacements were measured at the center on the top flange of the beam specimens. Two dial gauges were used to collect lateral deflections at the web mid depth of the beam specimens and track web buckling behaviors. Fig. 4 shows the testing setup. Digital videos and pictures were taken during the tests to capture the detailed time history of beam deformations.

2.4. Data collection

In this study, the built-in load sensor and vertical deflection sensor in the material testing system automatically collect and transfer data to the computer through the data collection software. The collected data can be exported for data processing. The load versus vertical deflection curves can be plotted and compared using the data collection software. The peak loads from these curves correspond to the onset of the web buckling failure, which represent the web bearing capacity as shown in Fig. 5. The peak loads from load versus vertical deflection curves for the beam specimens of different corrosion forms and degrees were

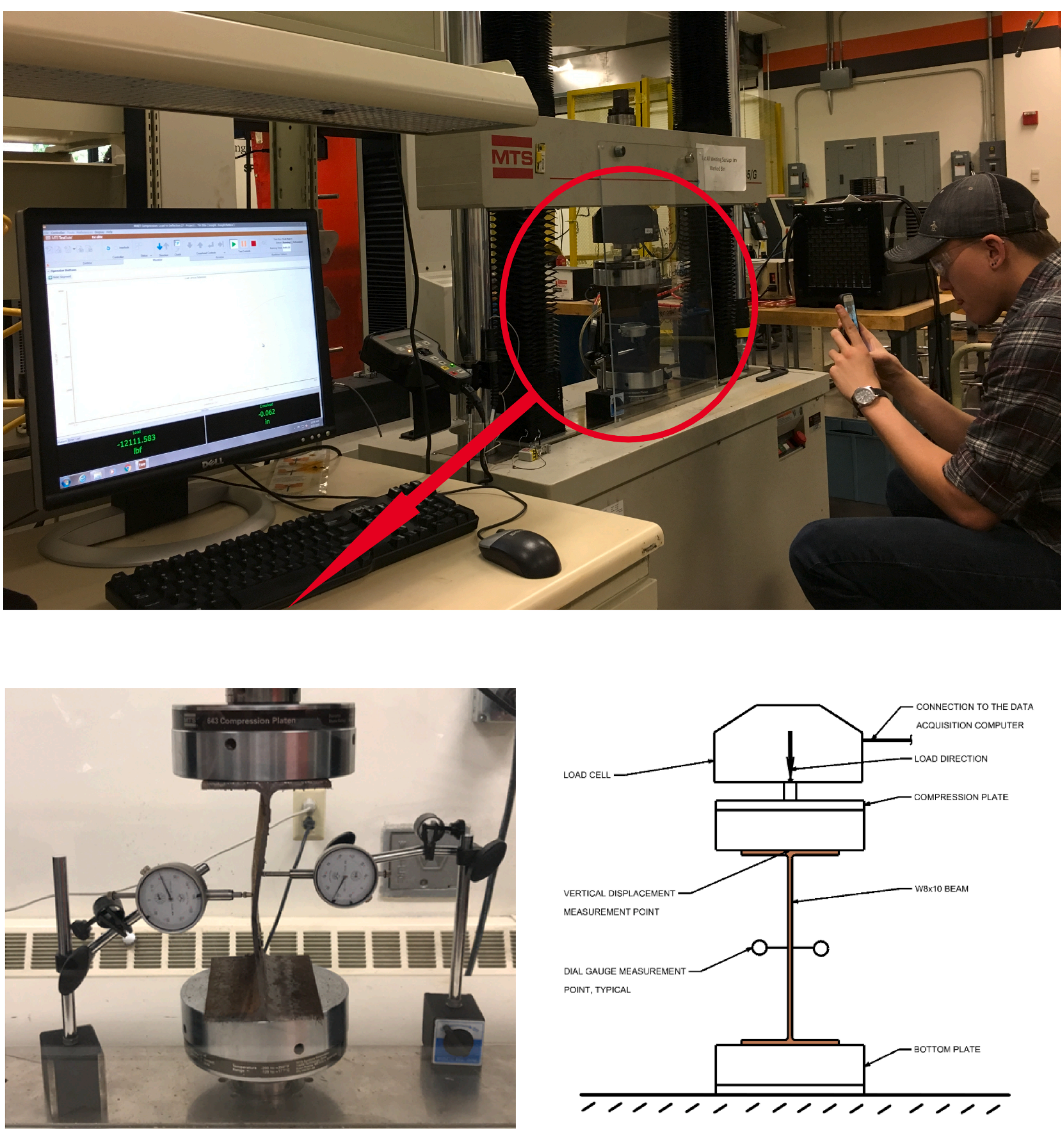

Fig. 4. Lab Testing Setup.

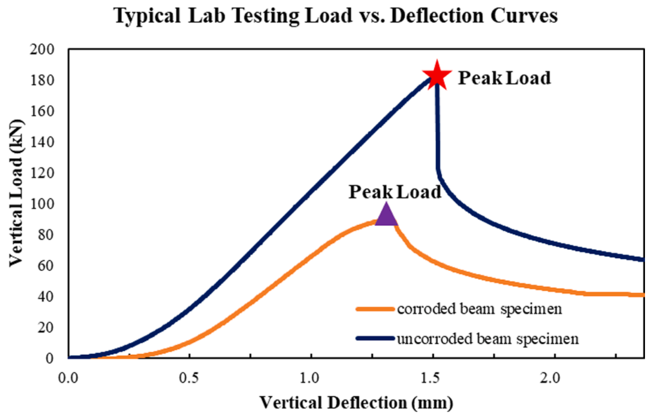

Fig. 5. Typical Lab Testing Load versus Vertical Deflection Curves.

compared and analyzed to investigate the relationship between web bearing strength and steel corrosion conditions.

The videos and pictures were taken during the testing procedure to track the real time history of beam specimens experiencing web buckling. The dial gauge readings immediately after web buckling, which was identified by the peak loads in the load versus deflection curves, were also recorded. The deformed shapes of the steel beam specimens subjected to web buckling failure are demonstrated in Fig. 6.

2.5. Testing results

After each test, the load versus vertical deflection numerical data was saved. The peak loads, namely the web bearing strength of the beam specimens, were recorded and plotted versus different corrosion forms in Figs. 7–9. For every data point plotted in Fig. 7, three beam specimens were tested and the differences of the testing results among the three beam specimens for the same data point were within 5%, and then the values were averaged. The web thinning percentages on the horizontal axis were obtained by dividing the web weight loss after corrosion by the specimen's web original weight. The peak loads on the vertical axis were selected directly from the test output files from the data collection software. There are 3 test data points in Fig. 7. The first point, (0%, 181.8kN), represents the intact beam strength and is used as the reference strength for other corroded beam specimens. The second point, (8.7%, 110.4 kN), represents moderate corrosion conditions for web thinning, and the third point, (14.8%, 91.3kN), represents severe web thinning. From Fig. 7, we can find that the peak load decreases significantly with the web thickness loss. At the third point, with 14.8% web thickness loss, the peak load was only 50.2% of its original strength. The trend of the testing results aligns with the classic buckling theory, in which the buckling strength is reported to be proportional to the web thickness cube.

Fig. 6. Deformed Steel Beam Specimens after Peak Loads in Lab Testing.

In order to study how holes in web affect the web bearing strength of the beam, a series of beam specimens with a rectangular hole cut from the web were tested. The first group of tests were only focused on hole sizes, so the beam specimens were prepared using the original beams without any web thinning. The hole sizes were 2.54 cm × 5.08 cm (1-in. × 2-in.), 2.54 cm × 7.62 cm (1-in. × 3-in.), 2.54 cm × 10.16 cm (1-in. × 4-in.), 5.08 cm × 5.08 cm (2-in. × 2-in.), 5.08 cm × 7.62 cm (2-in. × 3-in.) and 5.08 cm × 10.16 cm (2-in. × 4-in.), respectively. The bottom edges of the holes were at the interface between the bottom flange and the web (right above the fillet at the interface) to resemble the real corrosion form near the bottom flange as shown in Fig. 1, and the hole lengths were centered with respect to the vertical centerline of beam specimens. The testing results of holes sizes versus the web buckling strength are plotted in Fig. 8. There are 2 curves in Fig. 8. One is for the rectangular holes having the height of 2.54 cm, and the other curve shows the testing results of the beam specimens with holes of 5.08 cm height. The curve of 2.54 cm height holes is under the curve of 5.08 cm height holes, which indicates that with the same area of holes, the web bearing strength decreases at a faster rate when extending the hole in the direction parallel to the beam length than extending the hole parallel to the web depth. The testing results show that the aspect ratio of the perforation on the web significantly affects the web bearing strength. By inspection, the deformed specimens showed more localized buckling deformation occurred around the holes on the specimens of 2.54 cm height than the specimens of 5.08 cm height.

Fig. 9 shows the testing results of beam specimens with the combined corrosion forms of web thinning and holes. All the beam specimens had developed extensive web rust, and the web thickness losses were about 8.7%. Then, a rectangular hole, centered on the vertical centerline, was cut out of the web near the bottom flange for each beam specimen. The hole sizes were 2.54 cm × 5.08 cm (1 in. × 2 in.), 2.54 cm × 7.62 cm (1 in. × 3 in.), 2.54 cm × 10.16 cm (1 in. × 4 in.), 5.08 cm × 5.08 cm (2 in. × 2 in.), 5.08 cm × 7.62 cm (2 in. × 3 in.) and 5.08 cm × 10.16 cm (2 in. × 4 in.), respectively.

The results of combined corrosion forms in Fig. 9 show the same trend as Fig. 8. The curve of 2.54 cm (1 in.) height holes is under the curve of 5.08 cm (2 in.) height holes, which means that with the same web thickness loss and the same area of holes, the web bearing strength decreases at a faster rate when extending the hole in the direction parallel to the beam length than extending the hole parallel to the web depth.

3. Numerical modeling

3.1. Finite element model description

The ABAQUS three-dimensional finite element models were developed and calibrated against the performance of the beam specimens and then used as a tool to predict the performance of the prototype bridge girders, in order to study the web buckling behaviors of real deteriorated steel girders. Corrosive area loss was simulated by removing part of the web area, and web thinning was modeled by uniformly reducing the web thickness [3,4]. The three-dimensional finite element models were built to simulate the beam specimens in the lab testing. The models use the same dimensions as the W8x10 beam listed in Table 1. The length of the models is 15.24 cm. The steel material properties in the finite element models use the same properties as the W8x10 beam specimens described in Section 2.1. The elastic modulus is 200Gpa (29,000ksi) and the Poisson's ratio is 0.32. In this study, the corrosion forms were assumed to be fully modeled by removing the corroded materials from the original steel beam section, and the remaining steel section has the same properties as the original steel beam without corrosion. Therefore, the steel material properties keep constant in the finite element modeling.

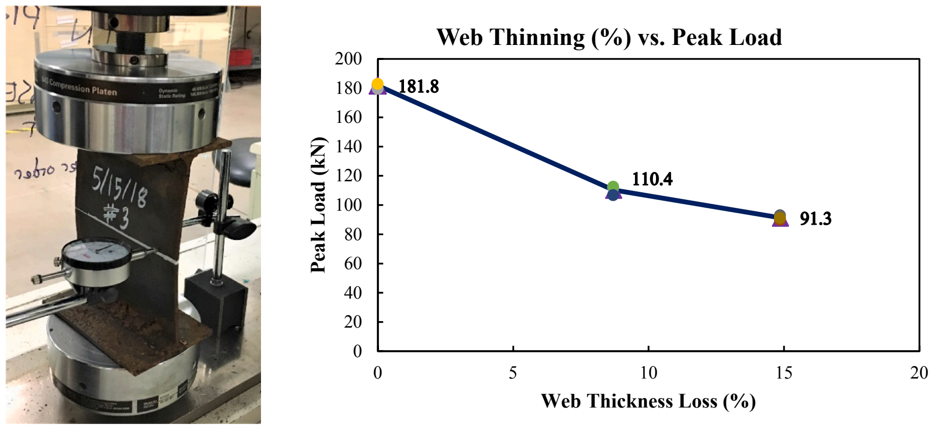

Fig. 7. Lab Testing Results of Web Bearing Strength versus Web Thinning.

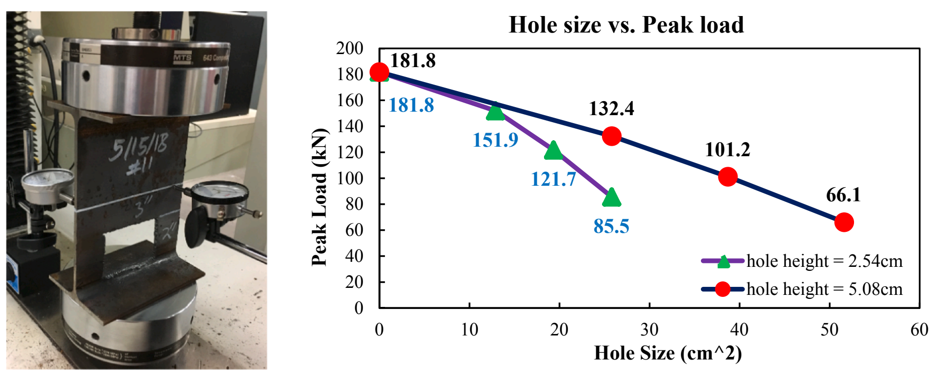

Fig. 8. Lab Testing Results of Web Bearing Strength versus Web Area Loss.

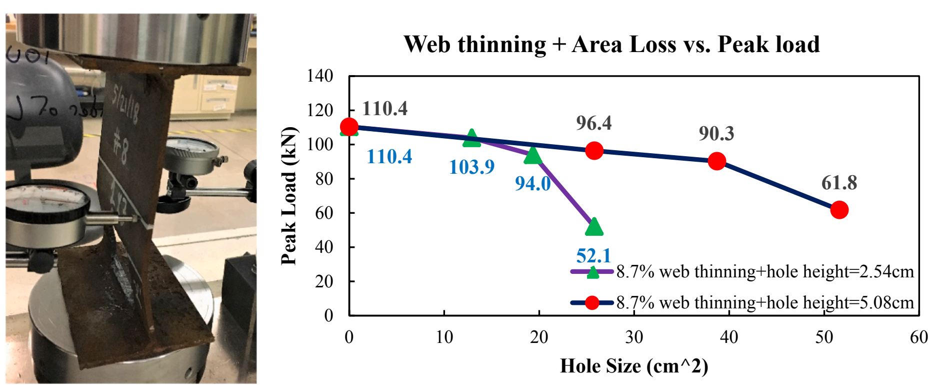

Fig. 9. Testing Web Bearing Strength for Combined Web Thinning and Web Area Loss.

3.2. Finite element modeling results for W8x10 steel beams

The numerical modeling results of web thinning and web holes are shown in Fig. 10 and Fig. 11, respectively, and the results are compared with the lab testing data. The web thinning effects were modeled at 0%, 5%, 10%, 15%, 20% and 25% in Fig. 10, which echoed the web thickness loss range with the 5% increment usually specified in bridge rating guidelines. In Fig. 11, the hole sizes used in the finite element modeling aligned with the beam specimens in lab testing as listed in Table 2: Group No. 2. Two additional data points were modeled in the numerical simulation: hole size of 2.54 cm × 12.70 cm and 5.08 cm × 12.70 cm to verify the trend.

The trend of the numerical modeling results was consistent with the lab testing data as shown in Fig. 10 and Fig. 11. The numerical models were then recalibrated by the data from the lab testing before being used to predict further theoretical behavior of steel bridge girders. The results for the web thinning simulation aligned with the lab data very well, and for the modeling results of steel beams with web holes, the differences between the numerical modeling and lab testing got larger when the hole sizes increased, and lab testing results had lower strength than the numerical modeling results. The causes of the differences can be:

1) Unlike the beam specimens used in the lab testing, the finite element models built in ABAQUS were elastic and were free of material, loading, or geometric imperfections and irregularities. Therefore, the numerical modeling tends to get higher strengths than the lab testing.

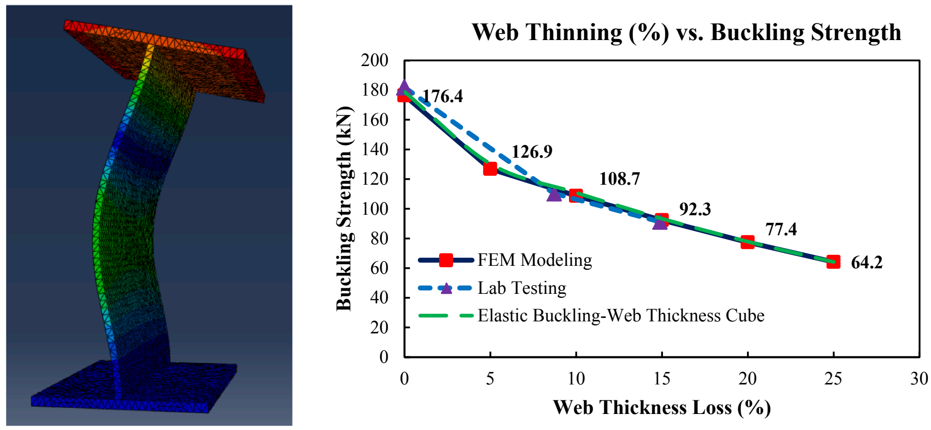

Fig. 10. W8x10 Modeling Web Bearing Strength versus Web Thinning.

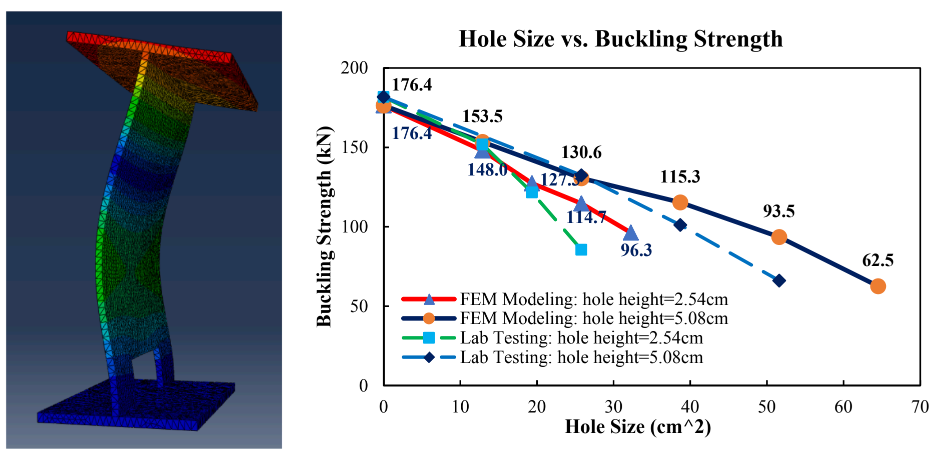

Fig. 11. W8x10 Modeling Web Bearing Strength versus Hole Sizes.

2) In the lab testing, the top flange was largely restricted to stay horizontal by the compression plate as shown in Fig. 7 and Fig. 8, but the numerical modeling buckling shape demonstrated some degree of top flange rotation as shown in Fig. 10 and Fig. 11. In the real-world, the top flanges of steel girders experience some degree of rotation under the vertical loads on the bridge, which is more similar to the numerical models.
3) In lab testing, the deformed shapes of the specimens with holes showed localized buckling deformation around the edges of the holes, which was not modeled and captured in the finite element models. Because of the difference, the numerical modeling for the steel beam with web holes still need further refined. In this study, the analysis will be focused on the trend of the web bearing strength with respect to the aspect ratio of the holes. More quantitative results and recommendations will be the future research work.

3.3. Finite element modeling results for large scale steel bridge girder

After successful comparison of W8x10 beam web buckling in a lab setting to that of a finite element model, a real size girder analysis was performed to study the web buckling behavior of a steel girder in a bridge. The prototype steel I-plate girder has a top flange of 30.48 cm (12 in.) wide and 5.08 cm thick, a web of 122 cm (48 in.) deep and 1.27 cm (½ inch) thick and a bottom flange of 30.48 cm wide and 5.08 cm thick. The initial web depth-to-thickness ratio of the prototype girder was 96. The overall depth of the steel girder is 132 cm (52 in.). The length of the girder end model is 254 cm (100 in.). The numerical models simulated the reactions at the girder end, and the boundary conditions simulated one end with the bearing pad under the bottom flange as pinned and the other end restrict the lateral displacements of the top and the bottom flanges. The bearing pad under the bottom flange is 15.24 cm (6 in.) long. The original web buckling capacity of the intact web was 3016 kN according to the ABAQUS analysis.

The web bearing strength versus web thinning is shown in Fig. 12. The web thicknesses in the plot are 1.27 cm (0.50-in., original thickness), 1.21 cm (0.475-in., 5% thickness reduction), 1.14 cm (0.45-in., 10% thickness reduction), 1.08 cm (0.425-in., 15% thickness reduction), 1.02 cm (0.40-in., 20% thickness reduction) and 0.95 cm (0.375-in., 25% thickness reduction), respectively. In Fig. 12, the horizontal axis is the percentage web thickness loss, and the vertical axis is the remaining percentage of the girder's original web buckling strength. The finite element modeling results are consistent with the trends shown in lab testing data. Moreover, in Fig. 12, the numerical modeling results were compared with the curve of the residual strength percentage based on the cube of the web thickness. The comparison shows the two curves align well, and indicates that the web bearing strength is closely related to the cube of the web thickness, which is consistent with the findings in the classic elastic buckling theory. In this study, the results for the web thinning corrosion form are consistent among the lab testing, numerical modeling on the steel beam specimens, numerical modeling on the large-scale steel girder as well as the classic elastic buckling theory. By combining these results, recommended values for bridge load rating of corroded steel girder bridges with web thinning are proposed in Section 4. The uniform web thinning in lab testing and numerical modeling reasonably simulated the typical corrosion form at the girder ends as shown in Fig. 1.

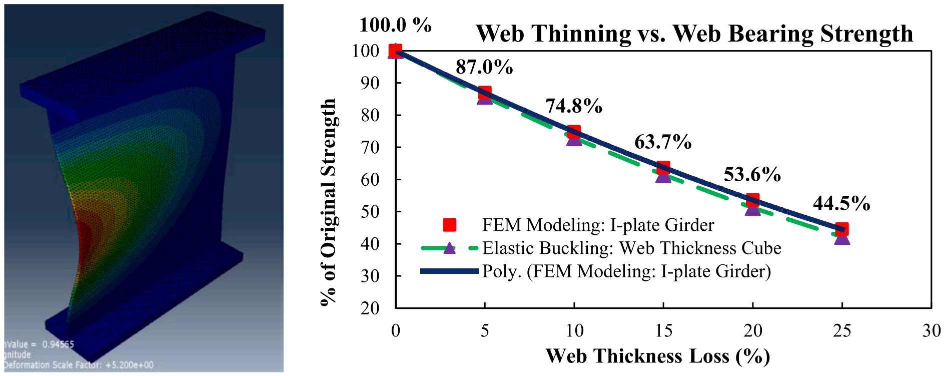

Fig. 12. I-Plate Girder Web Bearing Strength versus Web Thinning.

Following web thickness reduction studies, web holes were modeled by removing part of the web area. The hole heights of 7.62 cm (3-in.) and 15.24 cm (6-in.) were selected in the numerical models to represent the typical hole sizes in the real-world steel bridge girders. The results of web bearing strength versus hole sizes are shown in Fig. 13. The hole sizes in Fig. 13 for the 7.62 cm hole height were 7.62 cm × 38.10 cm, 7.62 cm × 45.72 cm, 7.62 cm × 53.34 cm, 7.62 cm × 60.96 cm, 7.62 cm × 68.58 cm, 7.62 cm × 76.20 cm, 7.62 cm × 83.82 cm and 7.62 cm × 91.44 cm, respectively; and the hole sizes for the 15.24 cm hole height were 15.24 cm × 15.24 cm, 15.24 cm × 38.10 cm, 15.24 cm × 45.72 cm, 15.24 cm × 53.34 cm, 15.24 cm × 60.96 cm, 15.24 cm × 68.58 cm, 15.24 cm × 76.20 cm, 15.24 cm × 83.82 cm and 15.24 cm × 91.44 cm, respectively. In Fig. 13, the horizontal axis is the area of the holes, and the vertical axis is the remaining percentage of the original girder's web bearing strength.

In Fig. 13, the numerical modeling results of the large-scale steel girder show the same trend as the lab testing results of the beam specimens. With the same area of holes, the web buckling strength decreases at a faster rate when extending the hole in the direction parallel to the beam length than in the direction parallel to the web depth.

Since the numerical models for the steel girder with web holes need further refined to account for local buckling effect around the holes, the analysis was focused on capturing the trend of web strength reduction.

4. Bridge load rating and proposed web bearing strength reduction factor

Bridge load rating is the main method adopted in the United States to evaluate the structural capacity of aging bridges [11,13]. Equation (1) is currently used to calculate loading rating factors for deteriorated steel girder bridges in practice [6].

$$RF = \frac{\varnothing_c \cdot \varnothing_s \cdot \varnothing \cdot R - \gamma_{DC} \cdot DC - \gamma_{DW} \cdot DW}{\gamma_L \cdot (LL + IM)} \tag{1}$$

where "*RF*" is the load rating factor of the girder, Φ_c is the condition factor, Φ_s is the system redundancy factor and Φ is the resistance factor. "*R*" is the structural capacity based on the member's dimensions and section properties. γ_{DC} is the load factor for the dead load and "*DC*" represents the dead load. γ_{DW} is the load factor for the wearing surface and "*DW*" represents the wearing surface. γ_L is the load factor for the live load, "*LL*" represents the live load and "*IM*" is the dynamic impact.

A deficient condition rating indicates deterioration at a level that requires corrective maintenance or rehabilitation to restore the bridge to its fully functional, non-deficient condition. The United States National Bridge Inventory (NBI) bridge condition rating guidelines are listed in Table 3. The Condition Factor Φ_c, does not account for section loss, but is used in addition to section loss to calculate the structural capacity of degraded members based on their conditions evaluated using the NBI condition rating system. The values of the condition factor Φ_c adopted in the current load rating procedure are listed in Table 4 [6].

System factors Φ_s listed in Table 5 [6] are multipliers to reflect the level of redundancy of the entire superstructure system in loading rating of steel members. The purpose of the system factor is to provide additional capacity for bridges with primary structural members that are non-redundant.

In order to facilitate application in bridge practices and be consistent with the existing load rating procedure in the United States, the proposed rating method will be based on the current load rating equation by introducing a web bearing strength reduction factor "*m*" as shown in Equation (2). According to the lab testing data and numerical modeling results in this paper, the web bearing strength reduction factor of deteriorated steel girders is proposed to account for web thinning. The modified structural capacity "$m \cdot R$" will be calculated to account for web material loss due to corrosion, where "*R*" is the original design section

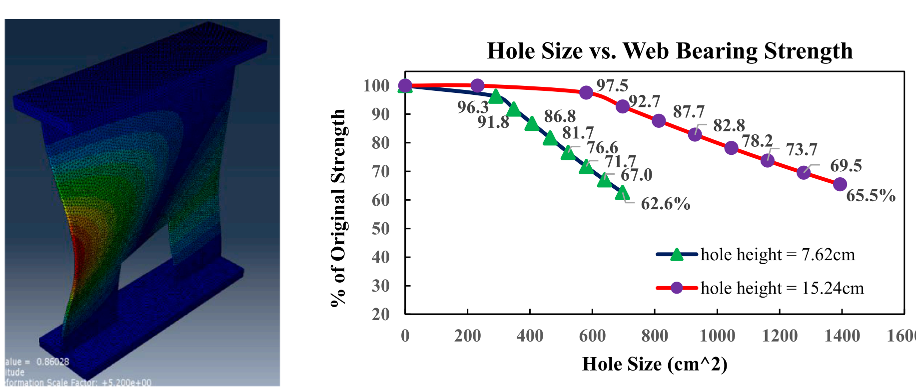

Fig. 13. I-Plate Girder Web Bearing Strength versus Hole Sizes.

Table 3
United States National Bridge Inventory Steel Bridge Condition Ratings [15,9].

Code	Condition	Description
9	New	No deficiencies in any of the structural components that will affect long term performance.
8	Very Good	All protective coatings are sound and functioning but with minor weathering of the coating.
7	Good	Very limited partial protective coating failures that do not expose bare steel. Members retain full section properties and function as designed with limited deterioration.
6	Satisfactory	Protective coating failures present with no loss of section. Members retain full section properties and function as designed with minor deterioration. Superficial impact damage.
5	Fair	Protective coating failures with minor loss of section. Cracks are arrested. All connections functioning as intended. Members continue to function as designed with moderate deterioration affecting structural members and minor section loss in low or no stress areas. Moderate impact damage that does not require mitigation.
4	Poor	Significant protective coating failure and limited loss of section. Cracks not arrested or missing fasteners are present. All members continue to function as designed with considerable deterioration affecting structural members and up to 10% section loss in scattered and isolated areas. Substantial impact damage may be present.
3	Serious	Protective coating failed with measurable loss of section. Cracks or missing fasteners may affect design capacity. Considerable deterioration affecting structural members and up to 25% section loss in scattered and isolated areas. Structural evaluation or load analysis may be necessary to determine if the structure can continue to function without restricted loading.
2	Critical	The superstructure will not support design loads. Posting, emergency repairs installed, or temporary shoring is required.
1	Imminent Failure	The bridge is closed to traffic due to the potential for superstructure failure, but corrective action may put it back in service.
0	Failed	The bridge is closed due to condition.
N	N/A	Not Applicable.

Table 4
Condition Factor Φ_c in Loading Rating [6].

Structural Condition of Member	NBI Code	Φ_c
Fair, Satisfactory, Good, Very Good, New	5–9	1.0
Poor, Serious, Critical, Severe, Failed	0–4	0.95

Table 5
System Factors used for Steel Girder Bridge Load Rating [6].

Superstructure Type	Φ_s
Welded members in two-girder bridges	0.85
Riveted or bolted members in two-girder bridges	0.90
All other girder bridges	1.00

Table 6
Proposed Web Bearing Strength Reduction Factor “*m*” in Load Rating.

Web Thickness Loss	Web Bearing Strength Reduction Factor “*m*”
1% inclusive – 3%	0.90
3% inclusive – 5%	0.80
5% inclusive – 8%	0.75
8% inclusive- 10%	0.70
10% inclusive –15%	0.60
15% inclusive- 20%	0.50
20% inclusive- 23%	0.40
23% inclusive- up to 25%	0.35

structural capacity. Recommended values of web bearing strength reduction factor “*m*” based on different deterioration conditions for I-plate steel girders are listed in Table 6. The recommendation values in Table 6 have taken conservative consideration of the differences between the lab testing results and numerical modeling results.

$$RF = \frac{\varnothing_c \cdot \varnothing_s \cdot \varnothing \cdot (m \cdot R) - \gamma_{DC} \cdot DC - \gamma_{DW} \cdot DW}{\gamma_L \cdot (LL + IM)} \tag{2}$$

5. Conclusions

In this paper, the residual web bearing strength of corroded steel beam specimens is tested and analyzed. The corrosion forms include the web thinning representing surface rust and the web hole representing localized rusted-through perforation. According to the lab testing and numerical modeling results, we can conclude that:

1) Web thinning due to corrosion not only reduces effective web cross sectional area, but also increases the depth to thickness ratio of the web, both of which contributes to the reduction in web bearing strength of the steel girder. Lab testing and numerical modeling results show that the residual web bearing strength of I-plate steel girders has correlation to the cube of the web thickness.
2) A quantitative relationship between corrosion condition and residual web bearing strength of I-plate steel girders is developed based on the laboratory testing and numerical modeling results. Recommended web bearing strength reduction factors are proposed to account for different levels of web thinning of corroded steel girders. Table 6 provides reference values for bridge load rating of deteriorated steel girders with web corrosion.
3) Holes forming in the girder web reduce effective web cross sectional area, which leads to web bearing strength reduction. Web bearing strength loss is proportional to the size of area loss. Moreover, the comparison between lab testing and numerical modeling results indicates that local buckling occurring around the holes could further reduce the web bearing capacity.
4) The aspect ratio of the hole in the steel girder web plays an important role in web bearing strength reduction. Web bearing strength decreases at higher rate when extending the area loss parallel to the girder longitudinal direction than extending the hole dimension parallel to the girder depth. This finding means holes extending longitudinally along the girder line have more concerns in web bearing strength reduction than holes extending vertically in the web near the girder ends, which may be use as a reference in bridge inspection and bridge load rating.

6. Further discussion

This paper was focused on the uniform web thinning and the localized web hole due to corrosion close to the girder bottom flange. Non-uniform web thinning was not covered in this paper; however, numerical modeling of non-uniform web thinning and lab testing will be the future research work. Future research needs also include modeling more realistic boundary conditions of steel girder end in bridges, performing non-linear analysis and lab testing on longer and larger sizes of beam specimens with and without transverse stiffeners.

CRediT authorship contribution statement

Amanda Bao: Supervision, Conceptualization, Methodology, Writing - original draft, Project administration. **Caleb Guillaume:** Investigation, Formal analysis, Validation, Visualization, Data curation. **Christopher Satter:** Investigation, Validation, Visualization, Data curation. **Alana Moraes:** Formal analysis, Validation, Visualization, Data curation, Writing - review & editing. **Peter Williams:** Investigation, Validation. **Tucker Kelly:** Investigation, Validation. **Ying Guo:**

Investigation.

Declaration of Competing Interest

The authors declare that they have no known competing financial interests or personal relationships that could have appeared to influence the work reported in this paper.

Acknowledgments

This study was supported by the Association for Bridge Construction and Design - Western New York Chapter (USA) Research Grant (2017-2019). Dr. Beth Carle, Dr. Alan Raisanen and Material Testing Lab manager Leslie Gregg from Rochester Institute of Technology offered great help with lab testing.

Appendix A. Supplementary material

Supplementary data to this article can be found online at https://doi.org/10.1016/j.engstruct.2021.112276.

References

[1] Agrawal A, Chen Z, Kawaguchi A. Bridge element deterioration rates, technical report (Project # C-01-51). USA: The City College of New York; 2009.
[2] Appuhamy JMRS, Kaita T, Ohga M. Development of an efficient maintenance strategy for corroded steel bridge infrastructures. J Bridge Eng 2013;18(6):464–75.
[3] Bao A, Guillaume C, Gulasey M, Levitova N, Moraes A, Satter C. Structural capacity analysis of corroded steel girder bridges. In: Proceedings of the 3rd International Conference on Civil, Structural and Transportation Engineering, Niagara Falls, Canada, June 10–12.
[4] Bao A, Guillaume C, Moraes A. Shear strength of deteriorated steel girders in multi-girder bridges. In: Proceedings of the 10th International Structural Engineering and Construction Conference - Interdependence between Structural Engineering and Construction Management, ISBN: 978-0-9960437-6-2, Chicago, IL, USA, May 20–25.
[5] Fernandez I, Bairán J, Marí A. 3D FEM model development from 3D optical measurement technique applied to corroded steel bars. Constr Build Mater 2016;124:519–32. https://doi.org/10.1016/j.conbuildmat.2016.07.133.
[6] Ghosn M, Miao F, Sivakumar B. Load Resistance Factor Rating (LRFR) in NYS. Technical Report. USA: The City University of New York; 2011.
[7] Guo X, Kang J, Zhu J. 3D cellular automata-based numerical simulation of atmospheric corrosion process on weathering steel. J Mater Civ Eng 2018;30:11. https://doi.org/10.1061/(ASCE)MT.1943-5533.0002502.
[8] Kayser J, Nowak A. Reliability of corroded steel girder bridges. Struct Saf 1989;6:53–63.
[9] Michigan State Department of Transportation, USA. Bridge Safety Inspection NBI Rating Guidelines; 2016. p.p.15.
[10] National Bridge Inventory, USA. Deficient Bridges by Superstructure Material; 2016. https://www.fhwa.dot.gov/bridge/nbi/no10/mat16.cfm.
[11] New York State Department of Transportation, USA. Bridge Inspection Manual; 2017. p.p.10.
[12] Nishikata A, Tada E, Zhu Q. Long-term monitoring of atmospheric corrosion at weathering steel bridges by an electrochemical impedance method. Corros Sci 2014;87:80–8. https://doi.org/10.1016/j.corsci.2014.06.007.
[13] Ohio State Department of Transportation, USA. Manual of Bridge Inspection; 2014. p.p.192.
[14] Sharifi Y. Residual web bearing capacity of corroded steel beams. Adv Steel Constr 2012;8(3):242–55.
[15] US Department of Transportation Federal Highway Administration. Recording and Coding Guide for the Structure Inventory and Appraisal of the Nation's Bridges. Report No. FHWA-PD-96-001; 1995. p.p.38.
[16] Van de Lindt J, Ahlborn T. Development of steel beam end deterioration guidelines. USA: Michigan Technological University; 2005.